CAPNOGRAM SLOPE AND VENTILATION DEAD SPACE PARAMETERS: COMPARISON OF MAINSTREAM AND SIDESTREAM TECHNIQUES

[1,2]Adam L Balogh, [2]Ferenc Petak, [2]Gergely H Fodor, [2]Jozsef Tolnai, [1]Zsofia Csorba, [1]Barna Babik

[1] Department of Anaesthesiology and Intensive Therapy, University of Szeged, 6 Semmelweis u. H-6725 Szeged, Hungary

[2] Department of Medical Physics and Informatics, University of Szeged, 9 Koranyi fasor, H-6720 Szeged, Hungary

Corresponding Author:
Ferenc Petak, PhD
Department of Medical Physics and Informatics
Korányi fasor 9, Hungary H-6720
Phone: +36 62 545077
FAX: +36 62 545077
Email: petak.ferenc@med.u-szeged.hu

Running Title: Mainstream and sidestream capnography

ABSTRACT

Background: Capnography may provide useful non-invasive bedside information concerning lung ventilation heterogeneity, ventilation-perfusion mismatch and metabolic status. Although the capnogram may be recorded by mainstream and sidestream techniques, the capnogram indices furnished by these approaches have previously not been systematically compared.

Methods: Simultaneous mainstream and sidestream time and volumetric capnography was performed in anaesthetized, mechanically ventilated patients undergoing elective heart surgery. Time capnography was used to assess the phase II ($S_{II,T}$) and III slopes ($S_{III,T}$). The volumetric method was applied to estimate phase II ($S_{II,V}$) and III slopes ($S_{III,V}$), together with the dead space values according to Fowler (V_{DF}), Bohr (V_{DB}) and Enghoff (V_{DE}) methods and the volume of CO_2 eliminated per breath (V_{CO_2}). The partial pressure of end-tidal CO_2 (P_{ETCO_2}) was registered.

Results: Excellent correlation and good agreement were observed in $S_{III,T}$ measured by the mainstream and sidestream techniques (ratio=1.05 (0.16), R^2=0.92, $p<0.0001$). While sidestream significantly underestimated V_{CO_2} and overestimated $S_{III,V}$ (1.32 (0.28), R^2=0.93, $p<0.0001$), V_{DF}, V_{DB} and V_{DE}, the agreement between mainstream and sidestream techniques in the difference between V_{DE} and V_{DB} reflecting the intrapulmonary shunt was excellent (0.97 (0.004), R^2=0.92, $p<0.0001$). P_{ETCO_2} exhibited good correlation and mild differences between the mainstream and sidestream approaches (0.025 (0.005) kPa).

Conclusions: Sidestream capnography provides adequate quantitative bedside information about uneven alveolar emptying and ventilation/perfusion mismatch, since it allows reliable assessments of the phase III slope, P_{ETCO_2} and intrapulmonary shunt. Reliable measurement of volumetric parameters (phase II slope, dead spaces and eliminated CO_2 volumes) requires the application of a mainstream device.

Key words: capnography, mechanical ventilation, ventilation perfusion mismatch, perioperative monitoring, carbon dioxide

INTRODUCTION

Capnography is a non-invasive method for the numerical and graphical analysis of the exhaled CO_2 concentration[1-5], and a valuable tool for the improvement of patient safety[6]. While assessment of capnogram shape factors is not standard part of the patient monitoring yet, they have the promise to possess routine information concerning pathophysiological processes of lung ventilation, such as airway patency[7-10] and lung recoil tendency[8 9]. Furthermore, combining capnography with expired gas volume monitoring allows the assessment of ventilation–perfusion matching and the metabolic status of the body[3 5 10 11].

In clinical practice, two techniques are available based on the measurement site of CO_2. Mainstream capnography applies an infrared sensor located proximally to the patient between the tracheal tube and the Y-piece and thus, allows a rapid and accurate analysis of the CO_2 concentration of the exhaled gas[12-14]. However, this method is used mainly in intensive care units, because of the disadvantages posed by the local heating of the head, and the weight of the sample cell increasing the risk of tracheal tube dislocation.

As an alternative, sidestream capnography is often used in the operating theatre because it is easily manageable and allows the monitoring of other gases[7-9 15]. These devices analyse the gas sample distally from the patient, and therefore have the drawbacks of a prolonged total response time[16-18], the occurrence of axial mixing[2 10 11 19] and a variable suction flow rate[20]. All these processes result in a dynamic distortion of the CO_2 concentration curve and thus, have a potential to bias the derived capnographic parameters.

There have been a few previous attempts to compare capnographic parameters obtained by sidestream and mainstream techniques, but they were either manufacturer's educational material[21], focused only on the end-tidal CO_2 value in experimental[22] and clinical studies[23-25], or were limited to a small cohort of infants[26]. However, there is a lack of information about

the relationship between capnographic indices obtained by sidestream and mainstream techniques in mechanically ventilated adults. Therefore, the aim of the present study was to validate the ability of the sidestream technique to provide adequate quantitative bedside information about uneven alveolar emptying and ventilation/perfusion mismatch. Therefore, we determined which of the capnogram parameters (shape factors, respiratory dead space) can be reliably assessed by applying the sidestream technique. We hypothesized that sidestream capnography is suitable to measure indices obtained from the quasi-static phases of the capnogram, whereas phases with transient CO_2 concentration changes are exposed to the measurement bias.

METHODS

Patients

Twenty-nine patients (female/male: 13/16, 71 (57-85) yrs) undergoing elective cardiac surgery were enrolled into the study in a prospective consecutive manner. The study protocol was approved by the Human Research Ethics Committee of the University of Szeged, Hungary (no. WHO 2788). Written informed consent was obtained from each patient. Patients with severe cardiopulmonary disorders (pleural effusion>300 ml, ejection fraction<30%, BMI>35 kg m^{-2} or intraoperative acute asthma exacerbation) were excluded.

Anaesthesia and surgery

Anaesthesia was induced with intravenous midazolam (30 μg kg^{-1}), sufentanil (0.4-0.5 μg kg^{-1}) and propofol (0.3–0.5 μg kg^{-1}), and was maintained by an intravenous propofol infusion (50 μg kg^{-1} min^{-1}. Neuromuscular blockade was achieved by intravenous boluses of rocuronium (0.2 mg kg^{-1} every 30 min).

After tracheal intubation, the patients' lungs were mechanically ventilated in volume-controlled mode with descending flow (Dräger Zeus, Lübeck, Germany) by setting the tidal

volume to 7 ml kg^{-1}, the ventilator frequency to 9–14 breaths per minute, and the positive end-expiratory pressure (PEEP) to 4 cmH_2O, and maintaining the inspired oxygen fraction (FiO_2) at 0.5.

Recording and analyses of the expiratory capnogram

The measurement setup was designed to allow the sampling of the mainstream (Novametrix, Capnogard®, Andover, MA, USA) and sidestream (Datex/Instrumentarium, Ultima™, Helsinki, Finland) capnographs from the same sampling site in the ventilator circuit. This was achieved by connecting the sampling port of the sidestream capnograph next to the mainstream sensor between the Y-piece and the tracheal tube. A screen pneumotachograph (Piston Ltd., Budapest, Hungary) was used to record the central airflow at the same point of the ventilator circuit. Simultaneous 15-s recordings of the CO_2 signals of the mainstream and sidestream capnographs and the ventilation flow were digitized (sampling frequency 102.4 Hz) and analysed with custom-made software. Volumetric capnograms were constructed from the time capnograms and the integrated flow data. To compensate for the transport delay caused by the suction of the gas into the sample cell, the sidestream time capnograms were shifted by -1.65 s. This value was determined by analysing the time delay between the mainstream and sidestream capnogram curves during stepwise changes in CO_2 concentration, similarly as in an earlier approach[17].

The slopes of phase III of the time and volumetric capnograms determined by mainstream ($S_{III,T,MS}$ and $S_{III,V,MS}$) and sidestream capnography ($S_{III,T,SS}$ and $S_{III,V,SS}$) were assessed by fitting a linear regression line to the last 60% of phase III[7 8 12]. Similarly, regression lines were fitted to the points around the inflexion point of phase II within ±20% of the time or volume of phase II, to determine their slopes in the mainstream ($S_{II,T,MS}$ and $S_{II,V,MS}$) and sidestream ($S_{II,T,SS}$ and $S_{II,V,SS}$) measurements. The angles formed by the phase II and III limbs of the

expiratory time mainstream (α_{MS}) and sidestream (α_{SS}) capnograms were calculated from the phase II and phase III slopes using a monitoring speed of 1.67 kPa s^{-1} (12.5 mmHg s^{-1}).

Additionally, dead space fractions were calculated from volumetric capnograms. Fowler's dead space, reflecting the volume of the conducting airways[27], was determined by taking the volume expired up to the inflexion point of phase II from the mainstream and sidestream capnograms ($V_{DF,MS}$ and $V_{DF,SS}$). The physiological dead space according to Bohr ($V_{DB,MS}$ and $V_{DB,SS}$) reflecting the alveolar volume with decreased or no perfusion was calculated from the mainstream and sidestream capnograms as[28]:

$V_{DB,MS}/V_T = (P_{ACO_2,MS} - P_{\bar{E}CO_2,MS})/P_{ACO_2,MS}$

$V_{DB,SS}/V_T = (P_{ACO_2,SS} - P_{\bar{E}CO_2,SS})/P_{ACO_2,SS}$

where $P_{ACO_2,MS}$ and $P_{ACO_2,SS}$ are the mean alveolar partial pressures of CO_2, determined from the midpoint of phase III in the mainstream and sidestream capnograms respectively [3 14]. $P_{\bar{E}CO_2,MS}$ and $P_{\bar{E}CO_2,SS}$ are the mixed expired CO_2 partial pressure, obtained by calculating the area under the mainstream and sidestream volumetric capnogram curves via integration and dividing the resulting values by V_T.

Enghoff's approach contains all of ventilation-perfusion mismatch. Hence, besides the V_{DB}, it also incorporates the intrapulmonary shunt, i.e. the alveolar volume with decreased or even loss of ventilation with perfusion maintained[29]:

$V_{DE,MS}/V_T = (P_{aCO_2} - P_{\bar{E}CO_2,MS})/P_{aCO_2}$

$V_{DE,SS}/V_T = (P_{aCO_2} - P_{\bar{E}CO_2,SS})/P_{aCO_2}$

where P_{aCO_2} is the partial pressure of CO_2 in the arterial blood.

Additionally we calculated the normalized differences between the Enghoff and Bohr dead spaces obtained by mainstream ($V_{s,MS}/V_T = [V_{DE,MS} - V_{DB,MS}]/V_T$) and sidestream capnography

($V_{s,SS}/V_T = [V_{DE,SS}–V_{DB,SS}]/V_T$), which reflects the all the mixed venous blood entering the arterial system. These include Thebesian veins, part of the bronchial veins and intrapulmonary shunt circulation, i.e. the virtual gas volume of the alveolar units with perfusion with decreased or no ventilation.

The amount of the CO_2 exhaled during each expiration was calculated as the area under the volumetric CO_2 concentration curve obtained by mainstream ($V_{CO_2,MS}$) and sidestream ($V_{CO_2,SS}$) capnography.

The changes in the sampling flow rate during the mechanical ventilation were measured in a smaller cohort of ventilated patients (n=5). The sampling flow was assessed by measuring the pressure difference between the proximal and distal ends of the sampling tube with a miniature differential pressure transducer (model 33NA002D, ICSensors, Milpitas, CA, USA). The potential variability of the sampling flow governed by the respiratory impedance can theoretically bias the accuracy of sidestream estimates. Thus, the main cohort of the patients were divided into three groups based on their compliance values into lower (C<37 ml cmH_2O^{-1}), higher (C>53 ml cmH_2O^{-1}) quartiles and medium interquartile range.

Measurement protocol

Mainstream and sidestream capnographic signals were recorded simultaneously during different stages of cardiac surgery: before sternotomy, 5 min before and after cardiopulmonary bypass, and immediately after sternal closure. Two pairs of 15-s traces were recorded in each stage, producing 8 recordings per patient (approximately 20 pairs of expirations). For the assessment of P_{aCO_2}, arterial blood gas samples were taken under each measurement condition, and the resistance (R) and compliance (C) values displayed by the ventilator were also registered.

Supplemental measurements

To assess whether sidestream capnography affects the mainstream results via gas suctioning, an additional protocol was performed with a setup identical to that used in the main study group in a smaller cohort of patients (n=8). A total number of 87 mainstream measurements, each lasting 60-s, were performed with the sidestream sampling flow switched on randomly during either the first or second half of the recordings. Separate analyses of first and second halves allowed pairwise comparisons of mainstream capnogram parameters obtained with and without gas suctioning by the sidestream device.

Statistical analyses

Sample size estimation was based on the aim to determine the 95% limits of agreement with great reliability according to the corresponding recommendation[30]. The correlations between the mainstream and sidestream variants of individual variables were analysed with the Pearson test. If the regression lines were close to the line of identity for a corresponding mainstream and sidestream value pair, Bland–Altman analysis was performed to assess the extent of their agreement[31]. In the event of normality, paired t-tests were used to assess the statistical significance of the difference between the results of the mainstream and sidestream methods. The effects of compliance on the sidestream and mainstream dead space and shunt parameters were assessed by using one-way ANOVA tests on ranks. A p value <0.05 was considered significant. The reported values are expressed as mean (SEM) in case of normality, or as median [1^{st} quartile–3^{rd} quartile] otherwise.

RESULTS

Figure 1 shows representative time and volumetric capnograms obtained with simultaneous mainstream and sidestream capnography. In both the time and volume domains the mainstream capnograms exhibited a steeper phase II, smaller α angles and an earlier transition

into phase III. Moreover, a later transition into the inspiratory phase was observed in the time domain mainstream capnogram. These shape differences result in a lower area under the sidestream capnograms as compared with the corresponding mainstream capnogram.

Figure 2 illustrates the temporal relationship between the sidestream capnogram and the sampling flow variability in a representative patient. The transient spikes in the sampling flow coincide with the cyclic changes in the breathing phases.

The difference in mainstream and sidestream P_{ETCO_2} (4.27 (0.02) vs. 4.24 (0.02) kPa) was small, although statistically significantly higher with the former technique ($p<0.001$). The V_{CO_2} was systematically underestimated by the sidestream method ($V_{CO_2,SS}/V_{CO_2,MS}=0.895$ (0.3), $p<0.0001$), despite the presence of good correlation between these variables ($R^2=0.91$, $p<0.0001$).

Correlations between the phase III slopes obtained by the mainstream and sidestream methods, and the corresponding Bland–Altman plots are demonstrated in Fig. 3. An excellent correlation ($R^2=0.92$, $p<0.0001$) and good agreement were observed between $S_{III,T,MS}$ and $S_{III,T,SS}$, although the sidestream method slightly but significantly overestimated $S_{III,T}$ ($S_{III,T,SS}/S_{III,T,MS}=1.05$ (0.16), $p<0.0001$). Strong correlation and good agreement were found between the volumetric S_{III} values ($R^2=0.93$, $p<0.0001$), with a systematic overestimation of $S_{III,V,MS}$ by $S_{III,V,SS}$ ($S_{III,V,SS}/S_{III,V,MS}=1.32$ [1.21–1.49], $p<0.0001$). The limits of agreements were -0.08 – 0.04 kPa s^{-1} and -0.07 – 1.16 kPa l^{-1} for the time and volumetric phase III slopes, respectively.

Figure 4 depicts the correlations between the shape factors and the dead space fractions associated with phase II of the capnogram (V_{DF}). Although $S_{II,T,SS}$ correlates significantly with $S_{II,T,MS}$ (R^2=0.58, p<0.0001), there is no agreement between these slopes because of the substantial underestimation by the sidestream method ($S_{II,T,SS}/S_{II,T,MS}$=0.48 (0.004), p<0.0001). A rather poor correlation and a lack of agreement were observed between the phase II slopes in the volume domain (R^2=0.02, p<0.002), with a similar underestimation by sidestream capnography ($S_{II,V,SS}/S_{II,V,MS}$=0.44 (0.008), p<0.0001). Significant correlation but poor agreement was found between the two types of α angle (R^2=0.89, p<0.0001), with α_{SS} slightly but consistently overestimating α_{MS} (1.04 (0.001), p<0.0001). Although $V_{DF,MS}$ and $V_{DF,SS}$ correlated moderately (R^2=0.56, p<0.0001), their agreement was rather poor, and the sidestream method overestimated the mainstream values ($V_{DF,SS}/V_{DF,MS}$=1.3 (0.013), p<0.0001).

Figure 5 illustrates the correlations between respiratory dead space indices measured by the two methods. Moderate, but statistically significant correlation was found between the normalized dead space parameters $V_{DB,MS}/V_T$ and $V_{DB,SS}/V_T$ (R^2=0.37, p<0.0001), with overestimation of mainstream Bohr's dead space by the sidestream method ($V_{DB,SS}/V_{DB,MS}$=1.37 (0.01), p<0.0001). In the measurement of the Enghoff dead space, the two methods exhibited good correlation (R^2=0.61, p<0.0001) and a slight overestimation by the sidestream capnograph ($V_{DE,SS}/V_{DE,MS}$=1.16 (0.004), p<0.0001). Since P_{ACO_2} shows excellent agreement between the two techniques (R^2=0.95 and mainstream/sidestream ratio=1.01 (0.02), p=0.2), the dissociations between physiological dead space parameters can be ascribed to the discrepancies in $P_{\bar{E}CO_2}$ (R^2=0.77 and mainstream/sidestream ratio=1.12 (0.08), p<0.0001). The overestimations of V_{DE} and V_{DB} by the sidestream technique resulted in a strong correlation in their difference (i.e. the lung volume with the intrapulmonary shunt;

R^2=0.92, p<0.0001 between $V_{s,SS}/V_T$ and $V_{s,MS}/V_T$). This relationship was associated with good agreement between the shunt volumes, with the sidestream method only slightly underestimating the mainstream values ($V_{s,SS}/V_{s,MS}$=0.97 (0.004), p<0.0001). The limit of agreement was 24 ml.

To reveal the effect of lung stiffness on the difference between the dead space and pulmonary shunt parameters determined by the mainstream and sidestream methods, Fig. 6 depicts the differences between mainstream and sidestream values as a function of C. Decreasing compliance resulted in an increasing overestimation of dead space and shunt parameters assessed by using the sidestream technique (p<0.0001).

In the supplemental measurements assessing the potential biasing effect of sidestream sampling flow on the mainstream parameters, no statistically significant differences were found in any of the mainstream capnogram parameters obtained with or without suctioning (Table 1; p>0.11), while a 3.64 (1.22) ml difference was found in V_T (p<0.004).

DISCUSSION

The results of the present study revealed that the sidestream capnography led to a dynamic distortion of the CO_2 concentration curve compared with the mainstream approach regarded as a reference technique[32]. Thus, the sidestream method biased the solid indices obtained from capnogram regions in which rapid changes in CO_2 concentration occur (i.e. phase II slopes, the transition from phase II to III, the end-tidal portion, V_{CO_2} and derived parameters such as Fowler's and Bohr's dead space). However, the sidestream technique does provide a good approximation of capnogram parameters characterizing periods of low rates of change in CO_2 (phase III slopes) and intrapulmonary shunt.

The differences between the sidestream and mainstream techniques can be explained by physical principles. The transport delay of the gas in the sampling tube is a well described characteristic of the sidestream measurement system[17]. This phenomenon introduces a predictable time lag in the detection of the CO_2 concentration, and gives rise to axial mixing of the gas residing in the sampling tube[2 10 11 19]. Axial in-line diffusion in both space and time occurs during the transport, depending on the CO_2 gradient[32]. This blurring process equilibrates the concentration differences between the gas compartments[26]. Theoretically, the biasing effects of this adverse process can be diminished by shortening the sampling tube and/or increasing the suction flow rate. Shortening the sampling tube (from 3 to 1.5 m) in 5 additional patients led to fairly proportional improvements in the sidestream estimates to the ratio of the tube lengths ($S_{II,T,SS}/S_{II,T,MS}$ of 37.4% and 60.2%; $V_{DF,SS}/V_{DF,MS}$ of 154.2% and 128.5% with long and short tubes, respectively). Similarly, increasing the sampling flow rate decreased the difference between sidestream and mainstream estimates ($S_{II,T,SS}/S_{II,T,MS}$ of 47% and 76%; $S_{III,T,SS}/S_{III,T,MS}$ of 146% and 99% for suction rates of 100 and 350 ml/min, respectively). These results suggest the possibility of improving the accuracy of shape factor estimates by using sidestream capnography.

A further factor contributing to the distortion of the sidestream capnogram is the variable sampling flow rate resulting from the alternating positive airway pressure during mechanical ventilation[19 20]. Since this phenomenon acts during inspiratory/expiratory phase transitions, it ultimately modifies the ascending and descending limbs of the capnograms[19 20].

The physical principles described above are of less importance in the assessment of the capnogram phase III slope. The reason for the good correlation and agreement (Fig. 3A, B) is the relatively steady-state CO_2 concentration (Fig. 1) and constant gas sampling flow during this period (Fig. 2). In the only previous study, where the sidestream and mainstream phase III

slopes were compared, substantially greater differences were observed in infants, which can be attributed to the higher ventilation rate (~32 min^{-1}) [26].

The initial part of the capnogram comprising the phase II slopes, angle α and V_{DF}, coincides with a high rate of change in the CO_2 concentration and with sudden pressure alterations in the breathing circuit causing variable sampling flow rate[20] in the tube of the sidestream capnograph. Consequently, in agreement with previous results on ventilated infants[26], the phase II slope of the sidestream capnogram is lower than that obtained by the mainstream technique (Fig. 1, bottom, Fig. 4B). This drop in $S_{II,T,SS}$ of necessity infers weak relationships between the anatomic dead spaces $V_{DF,MS}$ and $V_{DF,SS}$ (Fig. 4D), and the sidestream-derived α_{SS} (Fig. 4C).

The ventilation-perfusion mismatch can be divided into alveolar dead space ventilation and shunt perfusion[3] [14]. We obtained fairly weak correlations and agreements of both the normalized Bohr and Enghoff dead space fractions. The correlation analyses revealed that these dissociations can be ascribed to the discrepancies in the $P_{\bar{E}CO_2}$, resulting from the dynamic distortion of the sidestream capnogram (e.g. Fig. 1). Taking the difference between the Enghoff and Bohr dead spaces eliminates these discrepancies, which explains the excellent correlations and good agreement between $V_{s,MS}$ and $V_{s,SS}$ (Fig. 5C, D). The differences between the two estimates in the dead space and shunt parameters depend on the level of C, with greatest deviations in patients with low compliance (Fig. 6). Around the ventilation frequency, the respiratory system impedance is dominated by the elastic forces. Since low compliance involves higher airway pressures, variations in sampling flow rate are expected to be augmented within the respiratory cycle in the presence of increased stiffness. This implies that the use of dead space parameters determined by sidestream technique may result in false interpretations. Conversely, the assessment of the shunt fraction is feasible by

using sidestream capnography, though a slight underestimation is expected in patients with a less compliant respiratory system.

Our measurements demonstrate that the most frequently utilized capnogram parameter, the P_{ETCO_2}, is underestimated by a value with clinically minimal relevance (0.025 kPa). This concordance between the two techniques supports the conclusions of previous studies[23 25].

As a methodological aspect, we assessed whether gas sampling to the sidestream capnograph affects the shape of the mainstream capnogram resulting from the juxtaposed position of the mainstream sensor. However, the lack of differences in any of the mainstream parameters revealed that this effect has negligible impact on the mainstream parameters. This lack of sensitivity can also be anticipated from the amount of aspirated volume being about two orders of magnitude smaller than the V_T.

In conclusion, we evidenced that the sidestream capnography allows reliable measurement of P_{ETCO_2}, time and volumetric phase III slopes, and the intrapulmonary shunt fraction. Thus, sidestream capnography is suitable for quantification of the unevenness of the alveolar ventilation, and the ventilation-perfusion mismatch. However, reliable assessments of the phase II slope, the anatomical and physiological dead spaces, and the rate of elimination of CO_2 necessitate the combined application of mainstream volumetric capnography and sophisticated bedside information technology tools.

FUNDING

This work was supported by a Hungarian Scientific Research Grant (OTKA K81179 and K115253).

This research was supported by the European Union and the State of Hungary, co-financed by the European Social Fund in the framework of TÁMOP 4.2.6 ‘National Excellence Program’ and TÁMOP-4.2.2.D-15/1/KONV-2015-0024.

AUTHOR'S CONTRIBUTION

A.L.B.: acquisition, analysis and interpretation of data, writing up the paper; F.P.: study design, data analysis and writing up the paper; G.H.F.: analysis, interpretation of data, software design for data collection; J.T.: custom-made software design for data analysis, interpretation of data; Zs.Cs.: Patient recruitment, data collection; B.B.: Patient recruitment, analysis and interpretation of data, and writing up the paper. All authors contributed to revising the manuscript critically for important intellectual content.

FIGURE LEGENDS

Figure 1. Representative time (top) and volumetric (bottom) mainstream (continuous) and sidestream (dashed) capnograms.

Figure 2. Sidestream capnogram curve (solid line, left axis) together with the flow in the sampling tube (dashed line, right axis) in a representative patient.

Figure 3. Correlations between the phase III slopes in the time (**A**: $S_{III,T,MS}$ vs. $S_{III,T,SS}$) and volumetric domains (**C**: $S_{III,V,MS}$ vs. $S_{III,V,SS}$) obtained by mainstream (horizontal axis) and sidestream capnography (vertical axis) with the regression lines (dashed) and the lines of identity (continuous). Regression equations: $S_{III,T,SS}=0.142+0.996\cdot S_{III,T,MS}$ and $S_{III,V,SS}=5.09+0.93\cdot S_{III,V,MS}$.

The corresponding Bland–Altman plots are demonstrated on the right for the time (**B**: $S_{III,T,MS}$ vs. $S_{III,T,SS}$) and volumetric (**D**: $S_{III,V,MS}$ vs. $S_{III,V,SS}$) capnograms. The means of differences are -0.019 kPa s^{-1} and -0.55 kPa l^{-1} (continuous), and the limits of agreement are 0.06 kPa s^{-1} and 0.63 kPa l^{-1} (dashed) for the time and volumetric capnograms, respectively. Each data point represents one expiration.

Figure 4. Correlations between phase II slopes in the time (**A**: $S_{II,T,MS}$ vs. $S_{II,T,SS}$) and volume domain (**B**: $S_{II,V,MS}$ vs. $S_{II,V,SS}$), angles α (**C**: α_{MS} vs. α_{SS}) and Fowler's dead space indices obtained by mainstream (horizontal) and sidestream (vertical) capnography, with the regression lines (dashed) and the lines of identity (continuous). Regression equations: $S_{II,T,SS}=39+0.298\cdot S_{II,T,MS}$, $S_{II,V,SS}=140.2+0.1\cdot S_{II,V,MS}$, $\alpha_{SS}=-0.84+1.05\cdot\alpha_{MS}$ and $V_{DF,SS}/V_T=-22.3+1.52\cdot V_{DF,MS}/V_T$. Each data point represents one expiration.

Figure 5. Correlation between normalized dead space indices calculated according to Bohr (**A**: $V_{DB,MS}/V_T$ vs. $V_{DB,SS}/V_T$) and Enghoff (**B**: $V_{DE,MS}/V_T$ vs. $V_{DE,SS}/V_T$), and their difference (**C**: $V_{s,MS}/V_T=[V_{DE,MS}-V_{DB,MS}/V_T]$ vs. $V_{s,SS}/V_T=[V_{DE,SS}-V_{DB,SS}]/V_T$) obtained by mainstream (horizontal) and sidestream (vertical) capnography, with the regression line (dashed) and the

line of identity (continuous). Regression equations: $V_{DB,SS}/V_T=0.11+0.82\cdot V_{DB,MS}/V_T$, $V_{DE,SS}/V_T=0.12+0.86\cdot V_{DE,MS}/V_T$ and $V_{s,SS}/V_T=0.034+0.774\cdot V_{s,MS}/V_T$.

The corresponding Bland–Altman plot is demonstrated for $V_{s,MS}/V_T$ and $V_{s,SS}/V_T$ (**D**). The mean of differences is 6.17 (continuous), and the limit of agreement is 24.2 (dashed). Each data point represents one expiration.

Figure 6. Relative differences in dead space and pulmonary shunt parameters obtained with the two methods in patients with the lower (L, C<37 ml cmH_2O^{-1}), higher (H, C>53 ml cmH_2O^{-1}) quartiles and medium (M) interquartile range. *: $p<0.05$ vs. H; #: $p<0.05$ vs. M.

REFERENCES

1 Ortega R, Connor C, Kim S, Djang R, Patel K. Monitoring ventilation with capnography. *N Engl J Med* 2012; **367**: e27

2 Thompson JE, Jaffe MB. Capnographic waveforms in the mechanically ventilated patient. *Respir Care* 2005; **50**: 100-8; discussion 8-9

3 Tusman G, Sipmann FS, Bohm SH. Rationale of dead space measurement by volumetric capnography. *Anesth Analg* 2012; **114**: 866-74

4 Bhavani-Shankar K, Moseley H, Kumar AY, Delph Y. Capnometry and anaesthesia. *Can J Anaesth* 1992; **39**: 617-32

5 Walsh BK, Crotwell DN, Restrepo RD. Capnography/Capnometry during mechanical ventilation: 2011. *Respir Care* 2011; **56**: 503-9

6 American Society of Anesthesiologists. Standards for basic anesthetic monitoring. 2015. Available from http://www.asahq.org/~/media/Sites/ASAHQ/Files/Public/Resources/standards-guidelines/standards-for-basic-anesthetic-monitoring.pdf

7 Krauss B, Deykin A, Lam A, et al. Capnogram shape in obstructive lung disease. *Anesth Analg* 2005; **100**: 884-8

8 Babik B, Csorba Z, Czovek D, Mayr PN, Bogats G, Petak F. Effects of respiratory mechanics on the capnogram phases: importance of dynamic compliance of the respiratory system. *Crit Care* 2012; **16**: R177

9 Ioan I, Demoulin B, Duvivier C, et al. Frequency dependence of capnography in anesthetized rabbits. *Respir Physiol Neurobiol* 2014; **190**: 14-9

10 Stromberg NO, Gustafsson PM. Ventilation inhomogeneity assessed by nitrogen washout and ventilation-perfusion mismatch by capnography in stable and induced airway obstruction. *Pediatr Pulmonol* 2000; **29**: 94-102

11 Anderson CT, Breen PH. Carbon dioxide kinetics and capnography during critical care. *Crit Care* 2000; **4**: 207-15

12 Blanch L, Lucangelo U, Lopez-Aguilar J, Fernandez R, Romero PV. Volumetric capnography in patients with acute lung injury: effects of positive end-expiratory pressure. *Eur Respir J* 1999; **13**: 1048-54

13 Tusman G, Suarez-Sipmann F, Bohm SH, et al. Monitoring dead space during recruitment and PEEP titration in an experimental model. *Intensive Care Med* 2006; **32**: 1863-71

14 Tusman G, Sipmann FS, Borges JB, Hedenstierna G, Bohm SH. Validation of Bohr dead space measured by volumetric capnography. *Intensive Care Med* 2011; **37**: 870-4

15 Tusman G, Bohm SH, Sipmann FS, Maisch S. Lung recruitment improves the efficiency of ventilation and gas exchange during one-lung ventilation anesthesia. *Anesth Analg* 2004; **98**: 1604-9

16 Brunner JX, Westenskow DR. How the rise time of carbon dioxide analysers influences the accuracy of carbon dioxide measurements. *Br J Anaesth* 1988; **61**: 628-38

17 Breen PH, Mazumdar B, Skinner SC. Capnometer transport delay: measurement and clinical implications. *Anesth Analg* 1994; **78**: 584-6

18 Schena J, Thompson J, Crone RK. Mechanical influences on the capnogram. *Crit Care Med* 1984; **12**: 672-4

19 Epstein RA, Reznik AM, Epstein MA. Determinants of distortions in CO2 catheter sampling systems: a mathematical model. *Respir Physiol* 1980; **41**: 127-36

20 Farmery AD, Hahn CE. A method of reconstruction of clinical gas-analyzer signals corrupted by positive-pressure ventilation. *J Appl Physiol* 2001; **90**: 1282-90

21 Jaffe MB. Mainstream or Sidestream Capnography? *Respironics White Paper* 2002: 1012102 SB 8/23/02

22 Teixeira Neto FJ, Carregaro AB, Mannarino R, Cruz ML, Luna SP. Comparison of a sidestream capnograph and a mainstream capnograph in mechanically ventilated dogs. *J Am Vet Med Assoc* 2002; **221**: 1582-5

23 McEvedy BA, McLeod ME, Kirpalani H, Volgyesi GA, Lerman J. End-tidal carbon dioxide measurements in critically ill neonates: a comparison of side-stream and mainstream capnometers. *Can J Anaesth* 1990; **37**: 322-6

24 Pekdemir M, Cinar O, Yilmaz S, Yaka E, Yuksel M. Disparity between mainstream and sidestream end-tidal carbon dioxide values and arterial carbon dioxide levels. *Respir Care* 2013; **58**: 1152-6

25 Sakata DJ, Matsubara I, Gopalakrishnan NA, et al. Flow-through versus sidestream capnometry for detection of end tidal carbon dioxide in the sedated patient. *J Clin Monit Comput* 2009; **23**: 115-22

26 Pascucci RC, Schena JA, Thompson JE. Comparison of a sidestream and mainstream capnometer in infants. *Crit Care Med* 1989; **17**: 560-2

27 Fowler W. The respiratory dead space *Am J Physiol* 1948; **54**: 405-16

28 Bohr C. Über die Lungenatmung. *Skan Arch Physiol* 1891; **53**: 236-8

29 Enghoff H. Volumen inefficax. *Uppsala Laekareforen Forh* 1938; **44**

30 Bland M. How can I decide the sample size for a study of agreement between two methods of measurement? . 2004. Available from https://www-users.york.ac.uk/~mb55/meas/sizemeth.htm

31 Bland JM, Altman DG. Statistical methods for assessing agreement between two methods of clinical measurement. *Lancet* 1986; **1**: 307-10

32 Gravenstein JS, Jaffe MB, Gravenstein N, Paulus DA. Technical Perpectives. *Capnography*. Cambridge: Cambridge University Press, 2011; 381-96

Sidestream suctioning	$S_{III,T,MS}$ (kPa s^{-1})	$S_{III,V,MS}$ (kPa l^{-1})	$S_{II,T,MS}$ (kPa s^{-1})	$S_{II,V,MS}$ (kPa l^{-1})	$V_{DF,MS}/V_T$	$V_{DB,MS}/V_T$	$V_{DE,MS}/V_T$	$V_{s,MS}/V_T$	V_T (ml)
on	0.106 (0.108)	1.82 (0.92)	29.13 (5.42)	62.96 (14.31)	0.196 (0.037)	0.198 (0.04)	0.401 (0.059)	0.198 (0.067)	586 (116)
off	0.109 (0.104)	1.85 (0.92)	29.03 (5.36)	62.19 (14.23)	0.195 (0.036)	0.198 (0.04)	0.403 (0.058)	0.199 (0.065)	590 (116)
p-value	0.4	0.19	0.39	0.18	0.21	0.11	0.13	0.4	0.003

Table 1. Mainstream capnographic parameter values obtained with or without sidestream suctioning, and the corresponding p-values of paired t-tests. Values are expressed as mean (SD).

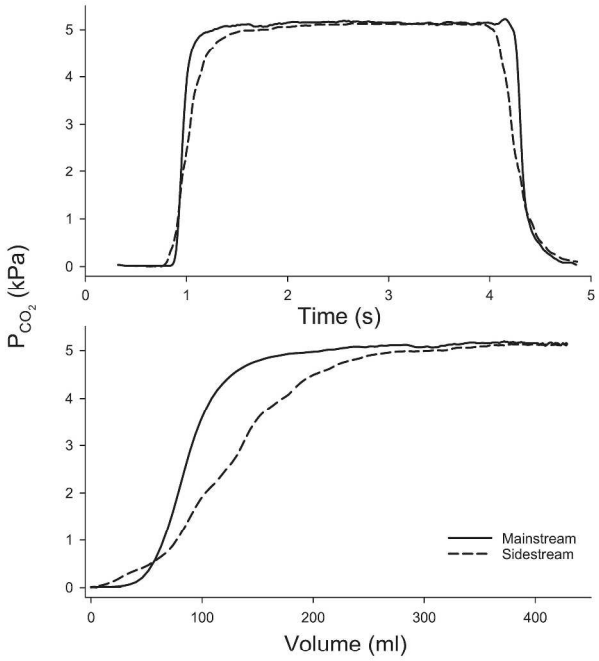

Figure 1

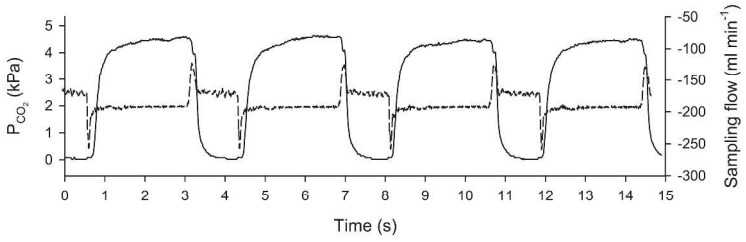
P_{CO_2} (kPa)
Sampling flow (ml min^{-1})
Time (s)
0
1
2
3
4
5
6
7
8
9
10
11
12
13
14
15
-50
-100
-150
-200
-250
-300

Figure 2

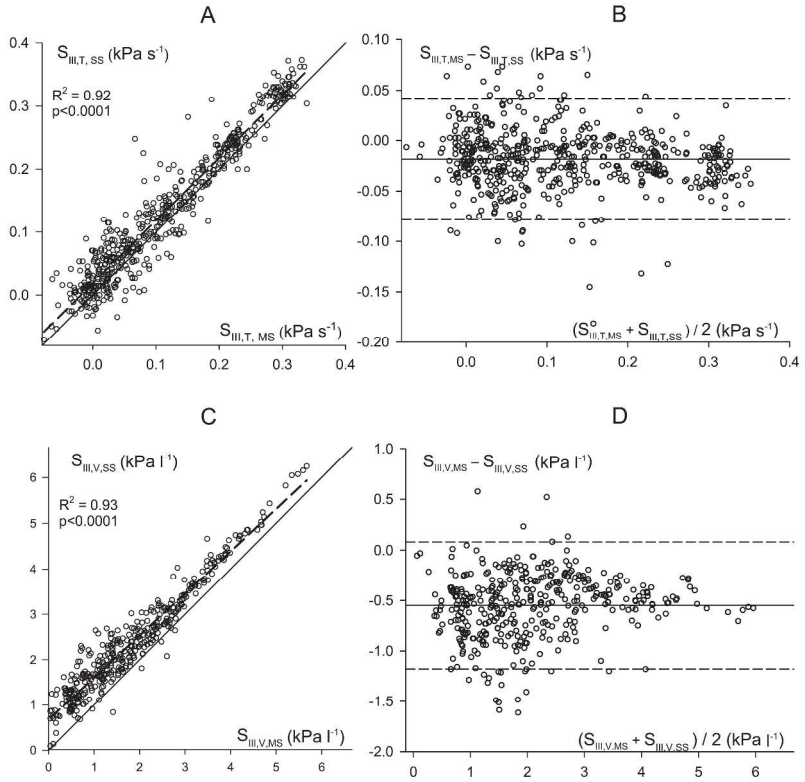
A
B
C
D
$S_{III,T,SS}$ (kPa s^{-1})
R^2 = 0.92
p<0.0001
$S_{III,T,MS}$ (kPa s^{-1})
$S_{III,T,MS} - S_{III,T,SS}$ (kPa s^{-1})
$(S^{\circ}_{III,T,MS} + S_{III,T,SS}) / 2$ (kPa s^{-1})
$S_{III,V,SS}$ (kPa l^{-1})
R^2 = 0.93
p<0.0001
$S_{III,V,MS}$ (kPa l^{-1})
$S_{III,V,MS} - S_{III,V,SS}$ (kPa l^{-1})
$(S_{III,V,MS} + S_{III,V,SS}) / 2$ (kPa l^{-1})

Figure 3

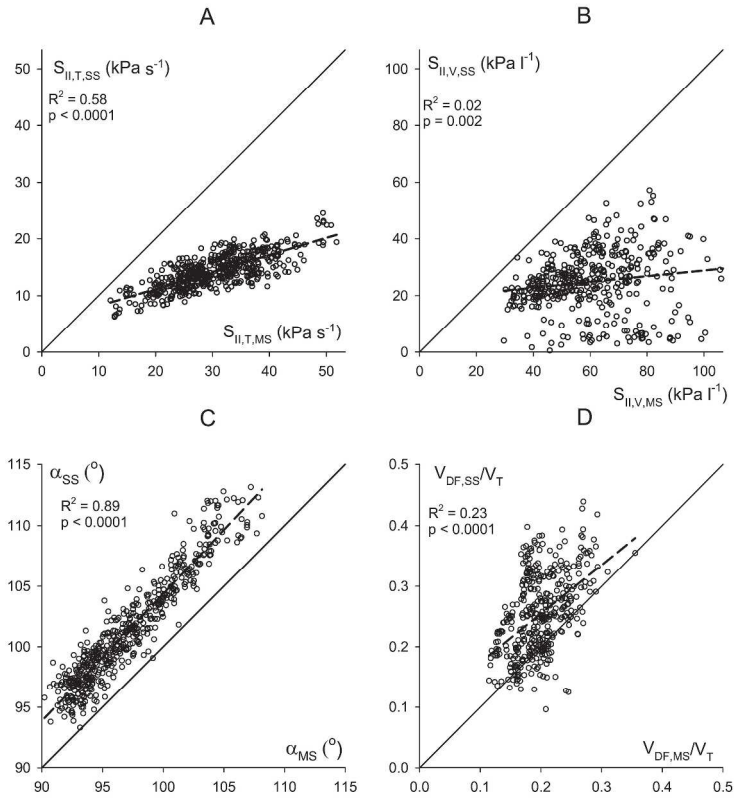
A
B
C
D
$S_{II,T,SS}$ (kPa s^{-1})
R^2 = 0.58
p < 0.0001
$S_{II,T,MS}$ (kPa s^{-1})
$S_{II,V,SS}$ (kPa l^{-1})
R^2 = 0.02
p = 0.002
$S_{II,V,MS}$ (kPa l^{-1})
α_{SS} (°)
R^2 = 0.89
p < 0.0001
α_{MS} (°)
$V_{DF,SS}/V_T$
R^2 = 0.23
p < 0.0001
$V_{DF,MS}/V_T$

Figure 4

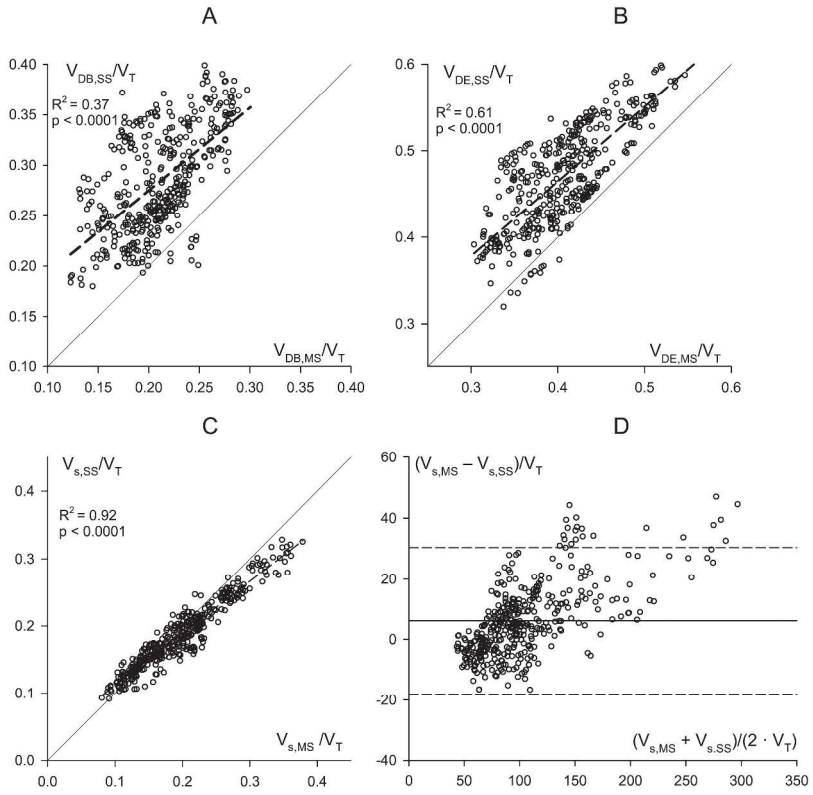
A
B
C
D
$V_{DB,SS}/V_T$
$R^2 = 0.37$
$p < 0.0001$
$V_{DB,MS}/V_T$
$V_{DE,SS}/V_T$
$R^2 = 0.61$
$p < 0.0001$
$V_{DE,MS}/V_T$
$V_{s,SS}/V_T$
$R^2 = 0.92$
$p < 0.0001$
$V_{s,MS}/V_T$
$(V_{s,MS} - V_{s,SS})/V_T$
$(V_{s,MS} + V_{s,SS})/(2 \cdot V_T)$

Figure 5

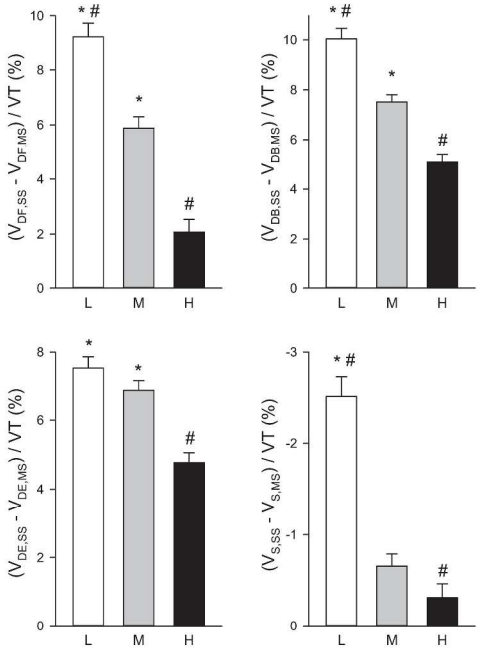

Figure 6